An Experimental Characterization of the PLC Noise at the Source

Massimo Antoniali, Fabio Versolatto, *Member, IEEE,* and Andrea M. Tonello *Senior Member, IEEE*

***Abstract*—Power line communications (PLC) are affected by severe noise. In the in-home scenario, the household appliances are the main sources of noise, when they are fed and running, as they inject noise in the frequencies where PLC operate.**

This work presents a methodology for the characterization of the noise generated by devices connected to the power grid. The methodology is applied to study a number of household appliances. The study enables to a) identify the most noisy devices from which PLC transceivers should be kept far away, b) characterize the noise both in the time and the frequency domain, c) address the definition of noise limits from an EMC regulator perspective, and d) quantify the amplitude of the impulsive noise that may damage the analog front-end of the PLC transceiver.

The work addresses both the noise during the normal operating conditions of the household appliances, and the noise generated during transients, i.e., when the device is connected, disconnected, switched on or off. In this respect, it is shown that transients may lead to noise spikes that exceed tens of Volts.

***Index Terms*—power line communications, impulsive noise, time-frequency analysis**

I. Introduction

The communication technologies that allow exploiting the power delivery network to convey data content are commonly referred to as power line communications (PLC). The power delivery network was not designed for communication purposes and thus PLC encounter several criticalities, as for instance, severe noise impairments [1].

From a PLC perspective, one of the most disruptive noise components is the differential-mode noise. In single phase networks, the differential-mode noise currents flow on the phase and neutral wires with the same intensity but opposite direction. Common-mode noise can also be present and it is generated by currents that flow with the same direction on both wires. Herein, we focus on the differential-mode noise.

The characterization of the PLC noise requires an extensive experimental activity that can be carried out either at the port where the receiver modem is connected or at the ports where the main sources of noise are connected. The former approach provides information about the overall noise that impairs the communication. The latter approach allows the characterization of the main sources of noise through the evaluation of the level of disturbance that they individually inject in a certain point of the grid.

A comprehensive characterization of the PLC noise at the receiver port was provided in [2]. It was shown that the PLC noise consists of background and impulsive noise components. The background noise is a combination of conducted and coupled noise contributions. The conducted noise contributions are amenable mostly to the devices connected to the power delivery network. The coupled noise contributions are due to the radio signals that are captured by the wirings. Typically, the background noise is modelled as stationary additive colored noise with a frequency decreasing power spectral density (PSD) profile. According to measures, the PSD decay profile can be modeled as a power function [3], or as an exponential function [4] of the frequency. Furthermore, the distribution of the amplitude in the time-domain can be fitted by the Middleton's class A [5] or the Nakagami-m distribution [6]. Some further studies reveal that the normal assumption on the noise statistics holds true if the periodic time-variant nature of the noise is accounted [7], and the impulsive noise contributions are removed from the noise measure [8].

The impulsive noise is unstationary and it can be a) cyclostationary with a repetition rate that is equal to or double that of the mains period, b) bursty and cyclostationary with a burst repetition rate that is high, between 50 and 200 kHz, or c) aperiodic. In the literature, the first two components are referred to as impulsive noise periodic synchronous and asynchronous with the mains frequency [9]. They exhibit a repetition rate equal or greater than the mains period. In particular, the periodic synchronous noise is originated by the silicon controlled rectifiers (SCR), while the asynchronous noise is due to, for instance, the switching activity of the power supplies. A time-frequency procedure to extract the periodic noise terms from the measures is presented in [8]. A model of the periodic noise terms that is based on a deseasonalized autoregressive moving average is discussed in [10].

The aperiodic noise is the most unpredictable component and it is due to the connection and disconnection of the appliances from the power delivery network. The amplitude of the aperiodic noise can be significantly larger than that of the other impulsive noise components. Beside the amplitude, the aperiodic impulsive noise is described by the duration and the inter-arrival time [11]. The statistics of these quantities depends on how the impulsive noise events are identified and measured. Several works addressed the characterization of the aperiodic impulsive noise. Among these, [9] proposes the use of a Markov-chain model to describe the same quantities in a combined fashion. Most of the papers above are focused on the frequency range up to 30 MHz.

The study of the PLC noise at the source is important for PLC technology manufacturers because it provides a clear indication about the devices that inject large noise components and that should be kept far from the PLC equipment. In a dual

Manuscript submitted on September 15, 2014, revised on January 9, 2015 and on March 24, 2015, accepted on June 14, 2015.
The work herein presented has been carried out in part at the University of Udine, Italy. The work of A. Tonello has been carried out at the University of Klagenfurt, Austria (e-mail: {massimo.antoniali, fabio.versolatto}@uniud.it, andrea.tonello@aau.at).

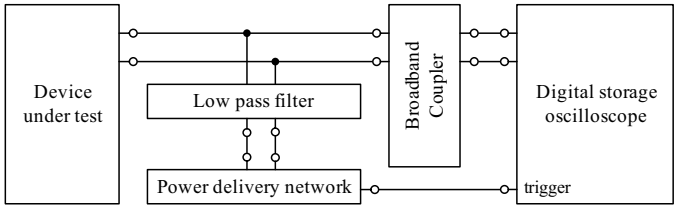

Fig. 1. Schematic representation of the measurement setup.

manner, the study of the PLC noise at the source is important for EMC regulation bodies as it provides guidelines for the definition of electromagnetic emission limits to enable the use of, and the coexistence with, PLC. Furthermore, the study of the noise at the source provides information on the maximum amplitude of the high-spikes of the aperiodic impulsive noise. This is fundamental for the design of the protection circuitry of the PLC equipment. Finally, we note that, from the measures of the noise at the source, we can obtain the noise at the receiver port by taking into account the effect of the channel response. This can be done by measuring the channel response or using a channel model. For instance, in [12] the noise at the source is modeled as in [3] and the channel response is obtained from a top-down modeling approach. Similarly, in [13] a top-down channel generator is used while the noise at the source is measured.

Some results about the noise at the source are presented in [14]-[15], although limited to the asynchronous impulsive noise. In particular, [14] shows noise spikes of up to thousands of Volts by switching on/off the devices, and [15] reveals noise spikes in the order of tens of Volts for the same events.

The goal of this work is to provide deeper insight on the noise at the source providing a statistical analysis of the results of an experimental measurement campaign that we carried out at the source, on real-life household appliances. Twelve representative household appliances were selected and the measurements were performed in the time domain. The database is well representative and it can be further extended with new measurement campaigns that share the measurement procedure and processing herein detailed. The processing enables separating the noise components and providing a characterization of each.

Compared to prior works in the literature, in this study, a) the frequency range is extended up to 100 MHz, b) an overview of all the noise components generated by the targeted devices is provided, and c) a novel characterization of the impulsive noise in power terms to account for both the amplitude and the duration of the noise spikes is presented.

The analysis allows to identify the intervals of the mains period during which the noise is higher, and the frequency intervals that experience the largest noise peaks. The peaks are amenable to either asynchronous noise components, that generate equally spaced peaks in the frequency [8], or other narrow band noise terms, as deterministic sinusoidal tones.

The remainder of the paper is organized as follows. Section II presents the rationale of the work, the scope, and puts the emphasis on the usefulness of the results. Section III describes the measurement configuration that we adopted. Sections IV and V deal with the noise observed during normal-mode operating conditions and during transient events, respectively. Finally, some conclusions follow.

II. Rationale

The study of the noise at the source is of great interest for PLC modem designers and EMC regulators. From a designer perspective, the noise at the source represents the worst-case noise scenario as it resembles an installation where the noise source is close to the transceiver, and its time/frequency domain analysis is useful to highlight the frequency bands and the time intervals during which the PLC transmission should be avoided or made more robust to cope with the noise impairments. Furthermore, the analysis of the impulsive noise amplitude and power is beneficial for the design of the protection circuitry of the analog front end.

From a regulatory perspective, the study of the noise at the source is important to understand the current emission of household appliances and their impact on PLC, and to draft new regulations that would limit further the noise emission in favor of PLC. For instance, not only during the normal-mode operating conditions, but also during transient events, as during switching on/off or plugging in/out a device.

III. Measurement Setup and Device Description

Fig. 1 shows the schematic representation of the time-domain measurement setup that we adopted. Basically, the digital storage oscilloscope (DSO) is connected close to the device under test (DUT). A broadband coupler protects the equipment from the mains, and a low pass filter (LPF) isolates the DUT from the rest of the power delivery network. The circuit design of the LPF resembles the electromagnetic compatibility filter of common appliances and it exhibits an attenuation in excess of 20 dB in the frequency range below 15 MHz, where the noise components coming from the network are mostly concentrated.

The resultant noise contribution due to the network is negligible. As a proof, Fig. 2 shows the PSD of the pure network noise, i.e., when the DUT is disconnected, and the PSD of the sum of the network and the DUT noise. For details about the PSD, see Section IV. As it can be noted, the noise generated by the DUT is larger that the pure network noise by more than 20 dB.

The setup is similar to that deployed in prior works in the literature. For instance, in [10], a fifth order stop-band passive filter is used to limit the noise in the frequency band 1-30 MHz. In [16], a commercial low-pass filter is deployed to stop the noise coming from the network. Alternatively, a line impedance stabilization network may be used instead of the low-pass filter [15], although the line impedance stabilization network performs well at frequencies up to 30 MHz.

A. Devices Under Test

In our analysis, twelve devices have been selected as representative of typical household appliances. They are listed in Table I. Three models of desktop PCs are considered in order to highlight, if any, differences between the noise injected

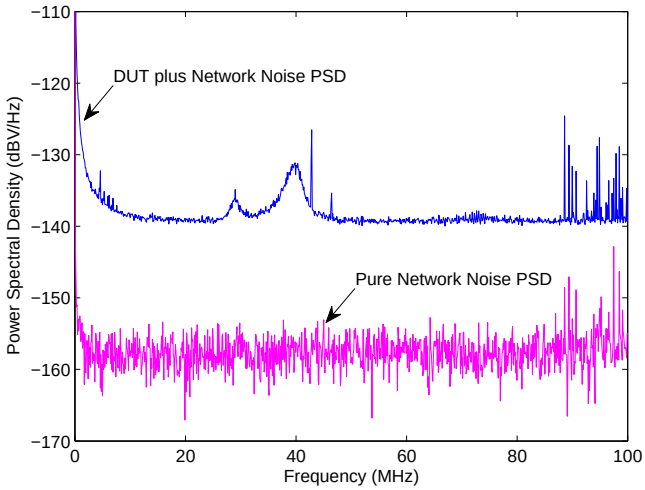

Fig. 2. Power spectral density of the pure network noise and of the pure network noise plus the DUT noise.

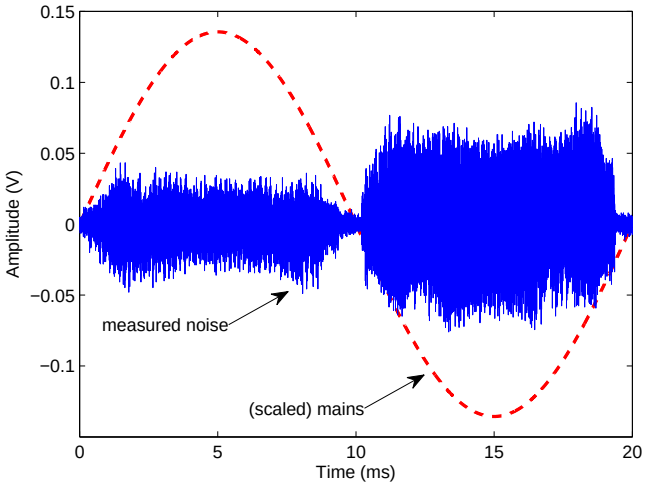

Fig. 3. Time-domain noise samples generated by device 9.

by their power supplies. The three PCs are distinguished by the letter A, B, or C and they are from different vendors. Furthermore, this study targets the noise injected by a light dimmer when it is set to supply half or a quarter of the maximum power. The results will show that the light dimmer injects large periodic noise components during short time periods of about 1 ms, whose position within the mains period is a function of the supplied power.

Beside the injected noise, a device is characterized by its impedance. The impedance of the device is important because it impacts on the PLC channel characteristics. As the noise, the device impedance can be time variant. Further, it depends on the state of the device. For instance, the vacuum cleaner exhibits an inductive or capacitive behavior when it is switched on or off, respectively [17]. The study of the device impedance is beyond the scope of this work and it is detailed in [17], [18].

IV. Normal-Mode Operating Condition

We now consider the noise injected by the household appliances during their normal operating conditions, i.e., when they are switched on and running. In particular, let us analyze the time-variant PSD. Measurements were performed as follows. The DSO was triggered to the mains cycle and it was configured to acquire an observation window equal to the mains period, i.e., 20 ms. The sampling period results from the ratio between the length of the observation window, i.e., $T_0 = 20$ ms, and the memory depth of the DSO which is equal to 10^7, yielding $T = 2$ ns. Hence, the sampling frequency is 500 MS/s. Such a high value was motivated, initially, by the purpose of exploring the noise in the maximum frequency band allowed by the instrument capabilities. As described in the following, results suggest that the noise is limited to the lower frequency band, below 20 MHz so that lower sampling frequencies can be used.

Finally, the input impedance of the DSO is set equal to 50 Ω. Fig. 3 shows a noise acquisition together with the (scaled) amplitude of the mains signal. We limit the study to the frequency range up to 100 MHz, namely, the band of practical interest for PLC purposes. The figure shows clearly the time variation of the noise signal.

In the following, we denote with $v^{(d)}(kT)$ the noise generated by the d-th device and acquired at the time instant kT, where d denotes the device index as in Table I, T is the sampling period and $k = 0, \ldots, K-1$, with K being the memory depth of the DSO ($K = 10^7$). The duration of the observation window is equal to the mains period, i.e., 20 ms, and C acquisitions of length equal to the observation window were performed for each device.

Now, we divide the observation window into I time intervals of duration T_0/I. We assume the noise to be stationary within each time interval. According to prior results in the literature and the experimental evidence, we chose $I = 20$ as a good trade-off between the resolution in time and frequency. A larger number of intervals is required when the noise is highly time-variant.

Finally, we introduce the notation $v^{(d)}(\ell, i, c)$, where $\ell = 0, 1, \ldots, L-1$ denotes the time instant within each time

TABLE I
Device under test and noise floor

d	Description	Noise Floor (dBV/Hz)
1	LCD flat monitor	-135
2	Satellite TV decoder	-150
3	Microwave oven	-150
4	Vacuum cleaner	-143
5	Laptop PC	-147
6	Desktop PC - model A	-143
7	Light dimmer (1/2 power)	-143
8	Light dimmer (1/4 power)	-143
9	Desktop PC - model B	-135
10	Desktop PC - model C	-135
11	Desk lamp	-150
12	Multifunction printer	-150

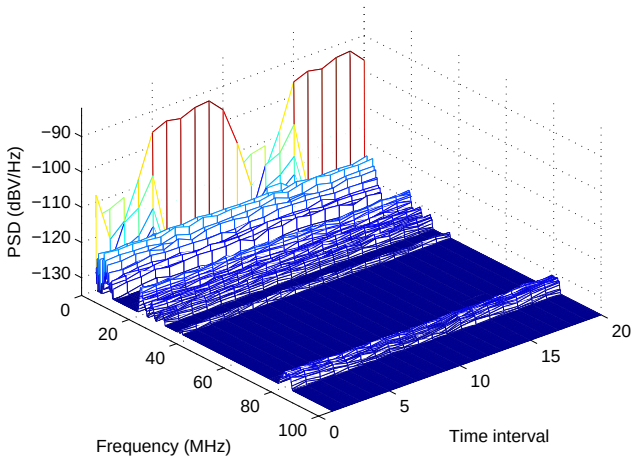

Fig. 4. Time-frequency representation of the effective noise PSD of the LCD flat monitor.

interval $i = 1, \ldots, I$, and $c = 1, \ldots, C$ denotes the acquisition. For each device, we perform $C = 200$ acquisitions of duration equal to the mains period. The acquisitions were not subsequent, but they were all synchronized with the mains period. Namely, they were spaced by an integer multiple of the mains period to let the DSO saving the acquired data.

In the frequency domain, we study the PSD of the noise. We obtain the PSD of the noise from the periodogram. However, we note that other analysis methods are possible as well. Among these, the wavelet transform spectrogram is one among the best alternative candidates.

The periodogram, as we define it herein, is the short time Fourier transform of the measured noise samples with no overlap between subsequent time intervals and assuming a rectangular window. The periodogram of the noise measure c of the device d, at the frequency sample n and time interval i reads

$$Q^{(d)}(n,i,c) = \frac{T}{L}\left|\sum_{\ell=0}^{L-1} v^{(d)}(\ell,i,c)e^{-j2\pi n\ell/L}\right|^2 \left[\frac{V^2}{Hz}\right], \quad (1)$$

where n denotes the frequency sample $f = n/LT$. The average of (1) on C acquisitions yields the PSD, i.e.,

$$P_v^{(d)}(n,i) = \frac{1}{C}\sum_{c=1}^{C} Q^{(d)}(n,i,c) \left[\frac{V^2}{Hz}\right]. \quad (2)$$

Specifically, the PSD of the noise generated by all the devices listed in Table I was computed as follows. Firstly, the noise generated by the power delivery network, namely, $P_{pd}^{(d)}(n,i)$, has been obtained measuring the noise of the pure network, i.e., without connecting any DUT. Similarly, $P_v^{(d)}(n,i)$ has been obtained measuring the noise with the DUT connected. Finally, the effective noise PSD (E-PSD), is given by the difference between the latter quantity and the contribution from the power delivery network, i.e.,

$$P_e^{(d)}(n,i) = P_v^{(d)}(n,i) - P_{pd}^{(d)}(n,i) \left[\frac{V^2}{Hz}\right]. \quad (3)$$

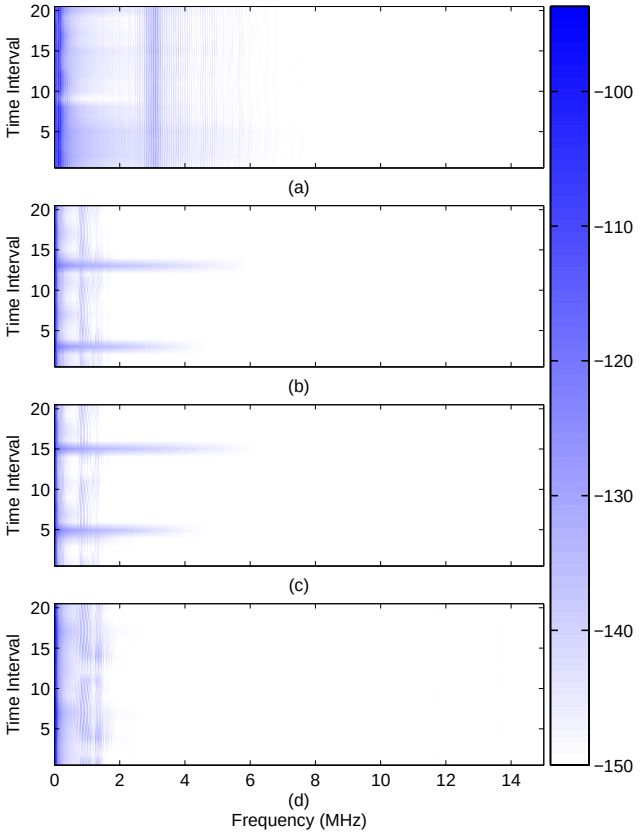

Fig. 5. From top to bottom, E-PSD of the devices 6, 7, 8, and 11 respectively.

All the quantities in (3) have been compute according to (2) on $C = 200$ acquisitions. Furthermore, relation (3) holds under the zero-mean assumption for all quantities and it is lower bounded by the noise floor of the DSO, i.e., the minimum measurable noise level. Note that the noise floor and $P_{pd}^{(d)}(n,i)$ must be estimated for all DUTs because the quantities depend on the y-axis settings of the DSO, and the latter has to be adjusted for each DUT in order to provide the best accuracy and to avoid clipping of the acquired noise signal. In addition, the noise coming from the network may vary between subsequent acquisitions. Table I reports the noise floor for each device in dBV/Hz.

Fig. 4 shows the E-PSD of device $d = 1$. Note that the noise contributions are mainly concentrated in the lower frequency range, i.e., below 15 MHz. Some minor contributions are observed between 20 and 40 MHz, and around 80 MHz. Furthermore, beside the noise contributions at very low frequencies, a negligible time variant behavior can be observed.

Fig. 5 reports the E-PSD in dBV/Hz of the most representative devices. The plots are limited to the frequency band up to 15 MHz, i.e., where most of the contributions are concentrated, regardless the device.

The analysis of the measured data offers the following conclusions. Firstly, the device that injects the highest levels of noise is a Desktop PC (model A) whose E-PSD is shown in Fig. 5(a). The PSD achieves -110 dBV/Hz, while the other devices do not exceed -120 dBV/Hz. Furthermore, the noise

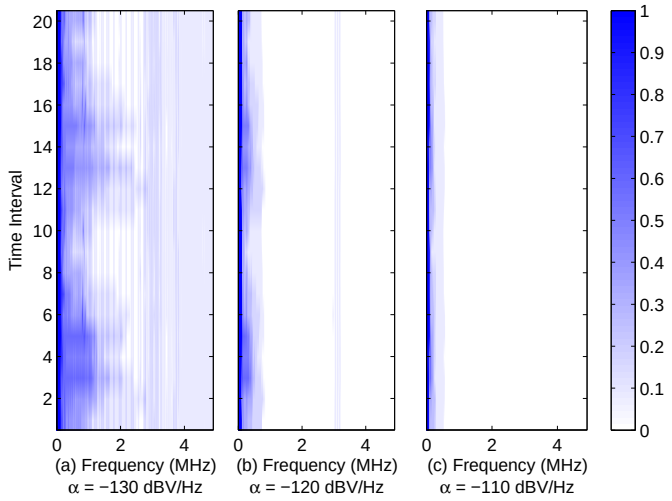

Fig. 6. From left to right, probability that P_{cyc} exceeds -130, -120 and -110 dBV/Hz, respectively.

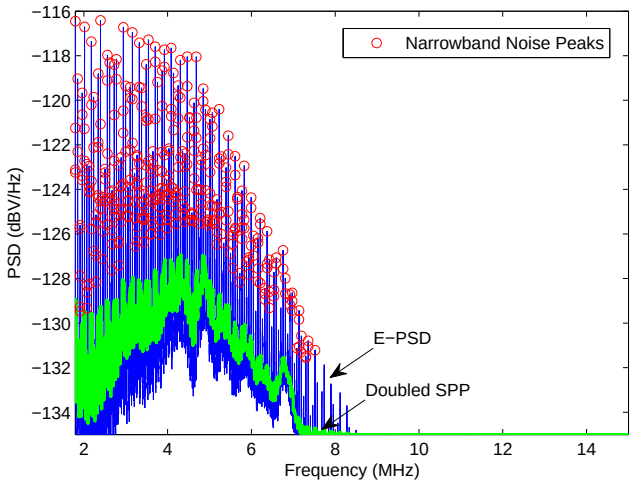

Fig. 7. E-PSD, doubled SPP and peaks associated to narrow band noise spikes of the LCD flat monitor at time interval $i = 19$.

injected by the other two PC models is significantly lower, say, below -122 dBV/Hz and, in the case of model B, it is confined to the 12-th time instant and the frequency range below 4 MHz. Secondly, the PSD of the dimmer depends on its regulation. From Figs. 5(b) - 5(c), it can be observed that the peaks of the PSD move to different time-intervals, when the dimmer is configured to deliver half or a quarter of the total available power. Furthermore, the noise of the dimmer is concentrated in few intervals and the maximum value is relatively low. Thirdly, the desk lamp does not inject noise above 1.8 MHz, as shown in Fig. 5(d). Finally, for most of the considered devices, the noise exceeds the floor only below 6 MHz.

A. Cyclostationary Behavior Analysis

In this section, we aim to check whether the noise is more concentrated in some time instants of the mains period. We focus on the mean PSD profile and its variations through the mains period. Namely, we study the cyclostationary noise component that exhibit a repetition period comparable to that of the mains. In this respect, we remove the narrow band peaks that are associated to noise components with high repetition rate and that are due to, for instance, the switching activity of the power supplies or deterministic sinusoidal tones. The narrow band peaks are identified according to the procedure described in Section IV-B and they are substituted with a linear interpolation of the PSD values in adjacent sub-bands. The result is denoted with $P_{cyc}^{(d)}(n,i)$.

To provide some insight of the results, we report the probability, computed merging the results from all devices, that $P_{cyc}^{(d)}(n,i)$ is larger than a threshold α at a certain time-frequency pair, i.e.,

$$\mathcal{P}(\alpha,n,i) = \text{Prob}[P_{cyc}^{(d)}(n,i) > \alpha] \tag{4}$$

Fig. 6 shows $\mathcal{P}(\alpha,n,i)$ for three values of α, i.e., -130, -120 and -110 dBV/Hz. The plots are limited to the frequency range below 5 MHz, where most of the contributions are concentrated. From Fig. 6(a), it can be noted that the time intervals between 2 and 6 and between 12 and 16 are affected by noise more than other intervals. They correspond to the peaks of the mains. Furthermore, from Figs. 6(b)-(c), we note that the noise rarely exceeds -120 dBV/Hz above 1 MHz.

B. Narrow Band Noise Peaks Analysis

To proceed in the analysis of narrow band noise components, the frequency associated to the peaks of $P_e^{(d)}(n,i)$ are identified according to the following criterion. Let us identify $\hat{n}$ as a frequency sample associated to a noise peak if $P_e^{(d)}(\hat{n},i) > 2P_m^{(d)}(\hat{n},i)$, where $P_m^{(d)}(\hat{n},i)$ is the smoothed PSD profile (SPP) computed as follows

$$P_m^{(d)}(n,i) = \frac{1}{N_r} P_e^{(d)}(i) * rect(n, N_r(n)), \tag{5}$$

with $rect(n, N_r(n))$ being a unitary vector of length $N_r(n)$,

$$N_r(n) = \begin{cases} 2n-1 & n < N_B/2, \\ 2(N_2-n)-1 & n > N_2 - N_B/2, \\ N_B & \text{otherwise}, \end{cases} \tag{6}$$

$N_2\Delta_f = 100$ MHz, and $N_B\Delta_f = 50$ kHz. As an example, Fig. 7 shows $2P_m^{(1)}(n,1)$, $P_e^{(1)}(n,1)$ and the peaks identified by the algorithm. Subsequent frequency samples that are identified as peaks determine a narrow band noise peak. Note that equally spaced PSD peaks correspond to noise terms that are periodic with a repetition period significantly smaller than the duration of the time interval of 1 ms. The literature refers to these noise terms as asynchronous periodic noise.

We extract the frequency intervals affected by narrow band noise for all devices and time intervals. Namely, a frequency sample can be (or not) affected by narrow band noise according to the proposed decision method. We combine the results from different devices to obtain the histogram of frequencies affected by narrow band noise. The histogram provides an indication on how many devices inject noise at a given frequency sample and time interval. We normalize the

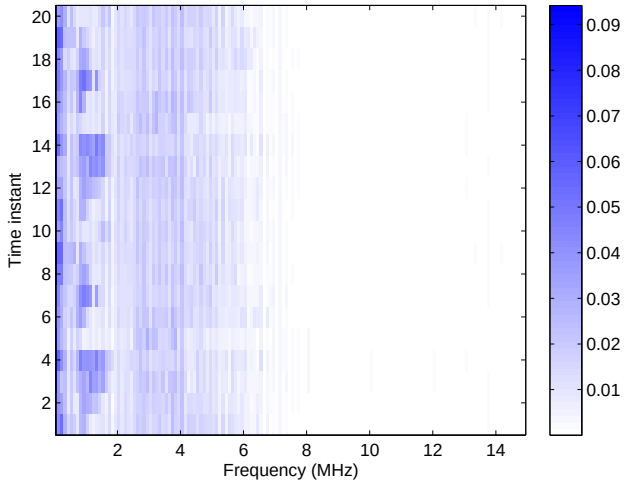

Fig. 8. Probability density function of the narrowband noise peaks.

histogram to obtain a probability density function (PDF). Fig. 8 shows the PDF as a function of the frequency and the time interval. The time-dependence of the PDF is negligible, the noise contributions are concentrated below 6 MHz and they do not dependent on the time instant. Furthermore, the highest values are below 4 MHz.

V. Aperiodic Noise

Connecting, disconnecting or switching on/off the devices may generate electric arcs that lead to aperiodic noise spikes. In this section, we characterize the maximum amplitude, the duration and the power of the aperiodic noise that is generated by the devices that are reported in Table I.

The measurements were carried out according to the time-domain setup described in Section III. The trigger was set to 200 mV, i.e., high enough to avoid acquiring the periodic noise. The sampling frequency is equal to 250 MHz and the number of acquired samples K is chosen to contain the aperiodic noise waveform in the shortest acquisition possible. Furthermore, the y-axis settings were adjusted to ensure the highest signal resolution in amplitude with negligible clipping effects. Finally, note that beyond 50 V, the acquisition is always clipped.

Tables II-III report the configurations of the DSO as a function of the device and the event. The configuration of the events that do not generate noise above the trigger level is not reported. The measure is repeated $R = 5$ times for each device and event. In most cases, the number of acquired samples is $K = 10^6$, i.e., an observation window of 4 ms, as the time required by the slowest noise waveform to approach the background noise amplitude.

We denote the acquisition of the d-th device and e-th event with $v^{(d,e)}(kT)$, where $e \in \{$plug in, plug out, switch on, switch off$\}$, and we study the maximum amplitude, the duration and the power of the noise waveforms. Firstly, let us focus on the amplitude. Table IV reports the maximum amplitude of the noise spikes for all devices and events. In all cases, the maximum value of the R acquisitions is provided.

TABLE II
DSO configurations for aperiodic noise acquisitions

Configuration	K (points)	Time length (ms)	Max amp. (V)
Conf. 1	10^6	4	50
Conf. 2	10^6	4	25
Conf. 3	10^5	0.4	50
Conf. 4	10^5	0.4	25
Conf. 5	10^5	0.4	10
Conf. 6	10^5	0.4	5
Conf. 7	10^3	0.04	10

Fig. 9 shows the most representative acquisitions of aperiodic noise in terms of amplitude, duration and power. The threshold amplitude that defines the impulse duration is also shown, and the waveforms refer to the devices and events whose statistics is detailed in Table V. The following observations can be made.

- The noisiest event is the plug-in event. All devices generate noise spikes greater than the threshold and that may even exceed 50 V. Some acquisitions reach the maximum amplitude allowed by the measurement configuration, as shown for instance in Fig. 9(a). In this respect, clipping is tolerated when the amplitude of the waveform exceeds slightly the maximum allowed value (the actual maximum amplitude of the measured signal has been checked before setting the optimal configuration of the DSO).
- Only devices 2, 7 and 9 generate noise spikes for a plug-out event.
- The on/off switching activity is noisy for the desktop lamp and the vacuum cleaner. They inject high noise spikes that may be due to the low-quality of the circuit breakers they are equipped with. The dimmer generates noise when a switch-on event occurs, but with lower values, namely, 6 V. All other devices do not exceed the trigger threshold.

Finally, the frequency domain analysis reveals that the

TABLE III
Configuration setup as a function of the DUT and the event

Device (d)	Event: plug-in	plug-out	switch-on	switch-off
1	Conf. 2	-	-	-
2	Conf. 4	Conf. 6	-	-
3	Conf. 3	-	-	-
4	Conf. 5	-	Conf. 3	Conf. 3
5	Conf. 3	-	-	-
6	Conf. 3	-	-	-
7	Conf. 7	Conf. 7	-	-
8	Conf. 7	-	Conf. 7	-
9	Conf. 3	Conf. 3	-	-
10	Conf. 3	-	-	-
11	Conf. 3	-	Conf. 1	Conf. 1
12	Conf. 3	-	-	-

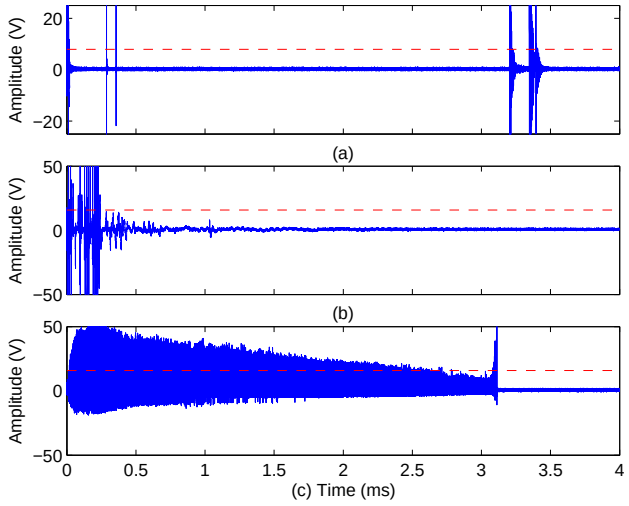

Fig. 9. From top to bottom, an example of the acquired impulsive noise generated by device 1 during plug in, device 6 during plug in, and device 11 during switch off.

aperiodic noise pulses spread over the broadband spectrum, with PSD levels that exceed -80 dBm/Hz below 10 MHz and -100 dBm/Hz at 30 MHz. Now, we study the duration of the noise spikes. Let us define the duration T_d as the distance between the first time instant, i.e., $k_1 T$, and the last time instant, i.e., $k_2 T$, for which the absolute value of the noise exceeds ρ times the maximum. We choose ρ = -10 dB.

Table IV reports the minimum, mean and maximum duration of the aperiodic noise for all operations and devices. The duration varies significantly even for noise waveforms generated by the same device and there is no clear indication about its behavior. To provide a description about the intensity of the bursty aperiodic noise, we study the power, namely,

$$P^{(d,e)} = \frac{1}{ZT_d} \sum_{k=k_1}^{k_2} T \left| v^{(d,e)}(kT) \right|^2 \quad [W], \qquad (7)$$

where Z = 50 Ω is the input impedance of the DSO. The evaluation of the noise power enables getting the real nature of the aperiodic noise components that are made by subsequent sparse spikes with amplitude exceeding the threshold for short intervals of time, as shown in Fig. 9(a).

Table IV reports the minimum, mean and maximum power of the measured noise. The power can be significantly high, but it refers to noise spikes with very short duration in time, i.e., less than 200 ns. In any case, the study highlights the disruptive nature of the impulsive noise. From a PLC modem manufacturer perspective, this implies, firstly, the need of protection circuits to preserve the analog front end, and, secondly, that the received signal is saturated by the impulsive noise so that the best option is to blank it to avoid corrupting the demodulation/decoding process.

VI. Conclusions

An experimental characterization of the PLC noise at the source has been herein presented. The work is based on the results of a measurement campaign that addressed the noise generated by a number of household appliances.

Both the noise generated during the normal-mode operating condition and during transients has been analyzed. The former is generated by the appliances during their normal activity, i.e., when they are switched on and running. The latter is generated when devices are switched on/off or they are plugged in/out. Concerning the normal-mode operation noise, we have firstly studied the cyclostationary behavior. Then, we have carried out an analysis of the frequencies where narrow band noise peaks are concentrated. The study has revealed the following findings.

- The noisiest device is a desktop PC that injects noise whose power spectral density exhibits peaks of up to -110 dBV/Hz, although below 4 MHz.
- In general, the noise shows a time variant behavior, with a period equal to the mains period.

TABLE IV
Characterization of the Aperiodic Noise

Id (d)	Ev. (e)	Amp. (V)	Duration (μs) min	avg	max	Power (mW) min	avg	max
1	p. in	25	0.62	1.3e3	3.4e3	18.5	153	471
2	p. in	25	0.66	34.4	81	65	1.6e3	3.6e3
	p. out	2	14	160	400	0.08	0.44	0.9
3	p. in	50	3.58	94	233	31	1.9e3	4.6e3
4	p. in	10	0.23	9.83	33.5	14.3	432	742
	s. on	50	0.17	25.3	86.6	609	6.7e3	2.5e4
	s. off	6.8	13.5	249	400	11.8	18	33
5	p. in	50	2.6	9.86	19.5	189	4.3e3	8.2e3
6	p. in	50	1.28	12.2	27.4	1.2e3	2.4e3	5.1e3
7	p. in	5	0.02	0.04	0.06	12.2	92.6	179
	p. out	5.8	0.05	1.95	4	2.12	42	143
8	p. in	3.84	0.03	0.46	2.1	0.54	56.2	87.2
	s. on	3.52	4e-3	2.26	4	0.36	88.3	310
9	p. in	50	0.58	15.5	36.5	186	3.2e3	7.2e3
	p. out	41.6	1.86	196	400	11.6	83.5	287
10	p. in	50	0.2	93.6	272	76.7	6.5e3	2.2e4
11	p. in	40.4	0.06	20.9	44.5	23.6	5.5e3	1.5e4
	s. on	50	354	395	443	54.8	637	1.1e3
	s. off	50	201	1.3e3	3.1e3	575	851	1.2e3
12	p. in	50	1.64	21.2	96.3	30.1	5.4e3	7.6e3

TABLE V
Characteristic of the Noise Waveforms

Fig.	Device (d)	Event (e)	Max. Amp. (V)	Duration (μs)	Power (mW)
9(a)	1	plug in	25	3.4e3	27.4
9(b)	6	plug in	50	24.1	5.1e3
9(c)	11	switch off	50	3.1e3	575

- Within the mains period, the noisiest time intervals are associated to time instants when the mains signal (in absolute value) reaches a peak.
- The narrow band noise is present below 4 MHz.

Finally, we have targeted the aperiodic noise that is generated during switching transients and we have shown that the aperiodic noise spikes may exhibit very large amplitudes, i.e., greater than 50 V, and they may last up to 4 ms, but with a low duty cycle. In fact, in general, the average power is small, in the order of fractions of Watts. Nevertheless, in all cases, the aperiodic noise is disruptive and blanking the received samples affected by such impairment is a valuable solution when combined with channel coding.

From a regulatory perspective, this study has highlighted that several devices inject a great deal of noise so that more PLC friendly norms should be developed by imposing more stringent EMC limits to power devices.

REFERENCES

[1] E. Biglieri, "Coding and modulation for a horrible channel," *IEEE Commun. Mag.*, vol. 41, no. 5, pp. 92–98, May 2003.
[2] M. Gotz, M. Rapp, and K. Doster, "Power line channel characteristics and their effect on communication system design," *IEEE Commun. Mag.*, vol. 42, no. 4, pp. 78–86, Apr. 2004.
[3] T. Esmailian, F. R. Kschischang, and P. Glenn Gulak, "In-building power lines as high-speed communication channels: Channel characterization and a test channel ensemble," *Intern. J. of Commun. Syst.*, vol. 16, no. 5, pp. 381–400, Jun. 2003.
[4] R. Hashmat, P. Pagani, and T. Chonavel, "Mimo communications for inhome plc networks: Measurements and results up to 100 mhz," in *Proc. IEEE Int. Symp. Power Line Commun. and Its App. (ISPLC)*, Apr. 2010, pp. 120–124.
[5] D. Middleton, "Statistical-physical models of electromagnetic interference," *IEEE Trans. Electromagn. Compat.*, vol. 19, no. 3, pp. 106–127, Aug. 1977.
[6] H. Meng, Y. L. Guan, and S. Chen, "Modeling and analysis of noise effects on broadband power-line communications," *IEEE Trans. Power Del.*, vol. 20, no. 2, pp. 630–637, Apr. 2005.
[7] M. Katayama, T. Yamazato, and H. Okada, "A mathematical model of noise in narrowband power line communication systems," *IEEE J. Sel. Areas Commun.*, vol. 24, no. 7, pp. 1267–1276, Jul. 2006.
[8] J. A. Cortés, L. Díez, F. J. Cañete, and J. J. Sánchez-Martínez, "Analysis of the indoor broadband power-line noise scenario," *IEEE Trans. Electromagn. Compat.*, vol. 52, no. 4, pp. 849–858, Nov. 2010.
[9] M. Zimmermann and K. Dostert, "Analysis and modeling of impulsive noise in broad-band powerline communications," *IEEE Trans. Electromagn. Compat.*, vol. 44, no. 1, pp. 249–258, Feb. 2002.
[10] F. Gianaroli, F. Pancaldi, E. Sironi, M. Vigilante, G. M. Vitetta, and A. Barbieri, "Statistical modeling of periodic impulsive noise in indoor power-line channels," *IEEE Trans. Power Del.*, vol. 27, no. 3, pp. 1276–1283, Jul. 2012.
[11] M. H. L. Chan and R. W. Donaldson, "Amplitude, width, and interarrival distributions for noise impulses on intrabuilding power line communication networks," *IEEE Trans. Electromagn. Compat.*, vol. 31, no. 3, pp. 320–323, Aug. 1989.
[12] L. di Bert, P. Caldera, D. Schwingshackl, and A. M. Tonello, "On noise modeling for power line communications," in *Proc. IEEE Int. Symp. on Power Line Commun. and Its App. (ISPLC)*, Apr. 2011, pp. 283–288.
[13] M. Tlich, H. Chaouche, A. Zeddam, and P. Pagani, "Novel approach for plc impulsive noise modelling," in *Proc. IEEE Int. Symp. on Power Line Commun. and Its App. (ISPLC)*, Mar. 2009, pp. 20–25.
[14] J. Khangosstar, L. Zhang, and A. Mehboob, "An experimental analysis in time and frequency domain of impulse noise over power lines," in *Proc. IEEE Int. Symp. on Power Line Commun. and Its App. (ISPLC)*, Apr. 2011, pp. 218–223.
[15] M. Tlich, H. Chaouche, A. Zeddam, and F. Gauthier, "Impulsive noise characterization at the source," in *Proc. IFIP Wireless Days WD'08*, Nov. 2008, pp. 1–6.
[16] J. J. Lee, S. J. Choi, H. M. Oh, W. T. Kee, K. H. Kim, and D. Y. Lee, "Measurements of the communications environment in medium voltage power distribution lines for wide-band power line communications," in *Proc. IEEE Int. Symp. Power Line Commun. and Its App. (ISPLC)*, Apr. 2004, pp. 69–74.
[17] M. Antoniali and A. M. Tonello, "Measurement and characterization of load impedances in home power line grids," *IEEE Trans. Instrum. Meas.*, vol. 63, no. 3, pp. 548–556, Mar. 2014.
[18] M. Antoniali, A. M. Tonello, and F. Versolatto, "A study on the optimal receiver impedance for snr maximization in broadband plc," *Journal of Electrical and Computer Engineering*, vol. 2013, pp. 1–13, 2013.

Massimo Antoniali received the B.Sc. degree in electrical engineering (2007), the M.Sc. degree in electrical engineering (2009, summa cum laude) and the Doctoral Degree in industrial and information technology (2013), all from the of University of Udine, Italy. In 2013 he joined SMS Concast Italia. His research interests are in the field of data communications and communication systems characterization. He received two best student paper awards at the IEEE International Symposium on Power Line Communications (ISPLC) in 2011 and in 2013.

Fabio Versolatto (SM10) received the B.Sc. degree (2007) and the M.Sc. degree (2009) in electrical engineering (both summa cum laude), and the Ph.D. degree in industrial and information engineering (2013), from the University of Udine, Udine, Italy. He was a member of the Wireless and Power Line Communications Lab at the University of Udine until 2015. Currently, he is with Innova, Italy. His research interests are in the field of channel modeling for power line communications and digital communication algorithms. He is member of the IEEE Technical Committee on Power Line Communications and he has been TPC member of IEEE ISPLC 2014. He received the best student paper award presented at IEEE ISPLC 2010.

Andrea M. Tonello (M00, SM12) obtained the Laurea degree (1996, summa cum laude) and the Doctor of Research degree in electronics and telecommunications (2003) from the University of Padova, Italy. From 1997 to 2002 he was with Bell Labs Lucent Technologies firstly as a Member of Technical Staff and then as a Technical Manager at the Advanced Wireless Technology Laboratory, Whippany, NJ and the Managing Director of the Bell Labs Italy division. In 2003 he joined the University of Udine, Italy, where he became Aggregate Professor in 2005 and Associate Professor in 2014. Herein, he founded the Wireless and Power Line Communication Lab. He also founded WiTiKee, a spinoff company in the field of telecommunications for the smart grid. Currently, he is the Chair of the Embedded Communication Systems group at the University of Klagenfurt, Austria. Dr. Tonello received the Lucent Bell Labs Recognition of Excellence award (1999), the Distinguished Visiting Fellowship from the Royal Academy of Engineering, UK (2010) and the Distinguished Lecturer Award by the IEEE Vehicular Technology Society (2011-13 and 2013-15). He also received (as co-author) five best paper awards. He is the Chair of the IEEE Communications Society Technical Committee on Power Line Communications. He serves an Associate Editor for the IEEE Transactions on Communications (since 2012) and IEEE Access (since 2013). He was the Chair of IEEE ISPLC 2011 and IEEE SmartGridComm 2014.